

Some reactions of an η^3 -tetracyanobutadienyl-ruthenium complex†

Michael I. Bruce,^{*a} Mark A. Fox,^b Paul J. Low,^b Brian W. Skelton^c and Natasha N. Zaitseva^a

Received 12th October 2009, Accepted 29th January 2010

First published as an Advance Article on the web 11th March 2010

DOI: 10.1039/b921324d

In the η^3 -butadienyl complex $\text{Ru}\{\eta^3\text{-C}(\text{CN})_2\text{CPhC}=\text{C}(\text{CN})_2\}(\text{PPh}_3)\text{Cp}$ **1**, which is formed from $\text{Ru}(\text{C}\equiv\text{CPh})(\text{PPh}_3)_2\text{Cp}$ and tene, a CN group reacts with MeO^- to give the methoxy-amide $\text{Ru}\{\text{NH}=\text{C}(\text{OMe})\text{C}(\text{CN})=\text{CCPh}=\text{C}(\text{CN})_2\}(\text{PPh}_3)\text{Cp}$ **2**, in which the NH has displaced the C=C from the Ru centre with formation of a RuC_3N ring. “Click addition” of azide to a CN group in **1** gives the oligomeric tetrazolato complex $\text{Ru}\{\text{N}_3\text{N}[\text{Na}(\text{OEt}_2)]=\text{CC}(\text{CN})=\text{CCPh}=\text{C}(\text{CN})_2\}(\text{PPh}_3)\text{Cp}$ **3**, also containing a RuC_3N ring. Salt-elimination reactions of **3** with MeOTf , $\text{FeCl}(\text{dppe})\text{Cp}$, $\text{RuCl}(\text{dppe})\text{Cp}^*$ and *trans*- $\text{PtCl}_2\{\text{P}(\text{tol})_3\}_2$ result in selective substitution at one nitrogen atom of the RuC_3N ring. Geometries of **1** and the anion in **3** were computed by DFT methods. Preferences for CN groups attacked in the nucleophilic and cycloaddition reactions of **1** are supported by NBO calculations. Alkylation of **1** in reactions with 1,2-dimethoxyethane gave two isomers of $\text{Ru}\{\text{N}_3[\text{CH}(\text{CH}_2\text{OMe})\text{-(OMe)}]\text{N}=\text{CC}(\text{CN})=\text{CCPh}=\text{C}(\text{CN})_2\}(\text{PPh}_3)\text{Cp}$ **8** and **9**, differing in the sites of attachment of the alkyl group, likely by radical processes. The molecular structures of eight complexes are reported, including a re-determination of **1**. Computed NMR chemical shifts are used to reassign the butadienyl carbon resonances in the ^{13}C NMR spectrum of **1**.

Introduction

After the initial report of the addition of the electron-poor olefin tetracyanoethene, $\text{C}_2(\text{CN})_4$ (tene), to alkynyl-iron complexes,¹ extensive studies with other transition metal alkynyl complexes showed that this reaction proceeds *via* an initial intensely-coloured radical species (presently structurally unidentified) to form the [2 + 2]-cycloadduct **A**, which then undergoes a more or less rapid ring-opening reaction to form an η^1 -butadienyl complex **B** (Scheme 1).^{2–10} If weakly bonded ligands are present on the metal centre, then displacement of one of these and chelation to give an η^3 -butadienyl **C** may occur.^{2,3,8,9,11–14} This type of reaction also occurs with related cyanoethenes such as $(\text{CF}_3)_2\text{C}=\text{C}(\text{CN})_2$,^{15,16} $\text{CH}(\text{CO}_2\text{Me})=\text{C}(\text{CO}_2\text{Me})\text{CN}$ ¹⁷ and $\text{PhCH}=\text{C}(\text{CN})_2$.^{18,19} As far as we are aware, the only reactions which have been reported for ruthenium complexes of type **C** are the addition of a ligand L' to give the η^1 -butadienyl **D**.^{3,11,19}

However, serendipitous hydrolysis or methanolysis of one of the CN groups has also been found to occur with the related complexes $\text{W}\{\text{C}(\text{CY}=\text{CX}_2)=\text{C}(\text{CN})_2\}(\text{CO})_3\text{Cp}$ ($\text{X} = \text{CF}_3$, $\text{Y} = \text{Ph}$ or $\text{X} = \text{CN}$, $\text{Y} = \text{Fc}$) of type **B** to give the five-membered metallacyclic complexes of type $\text{W}\{\text{NH}=\text{C}(\text{OR})\text{C}(\text{CN})=\text{C}(\text{CY}=\text{CX}_2)\}(\text{CO})_2\text{Cp}$ ($\text{R} = \text{H}$ or Me ; Scheme 2).^{7,15} Similar cyclic complexes $\text{M}\{\text{NH}=\text{C}(\text{OH})\text{C}(\text{CN})=\text{CH}\}(\text{CO})_2\text{Cp}$ ($\text{M} = \text{Mo}$, W) have been obtained from hydrolysis of $\text{M}\{\text{CCl}=\text{C}(\text{CN})_2\}(\text{CO})_3\text{Cp}$.²⁰

The reaction between tene and $\text{Ru}(\text{C}\equiv\text{CPh})(\text{PPh}_3)_2\text{Cp}$ affords directly the η^3 -butadienyl **1** (complex **C** in Scheme 1) in high yield (Scheme 3).¹¹ In this paper we describe an investigation into some chemistry of **1** with a view to discover further examples of cyclic complexes. We have re-determined the structure of **1** using a polymorph which does not exhibit the disorder found initially and have carried out DFT studies on complex **1** and some of its reaction products.

Results

The extensive chemistry of tene includes many examples of the characteristic nucleophilic displacement of one or two CN groups by alcohols, thiols, amines and similar reagents.^{21–23} Consequently, our first foray into the chemistry of **1** involved a study of its reaction with sodium methoxide. The reaction between **1** and NaOMe , carried out in a MeOH – thf mixture, resulted in a slow colour change from yellow to red-brown over a period of 48 h at r.t. Conventional work-up afforded dark red crystals of the cyclic amido derivative $\text{Ru}\{\text{NHC}(\text{OMe})\text{C}(\text{CN})=\text{CCPh}=\text{C}(\text{CN})_2\}(\text{PPh}_3)\text{Cp}$ **2** (Scheme 3) in 72% yield. This compound was characterised by a single-crystal X-ray structural determination while the elemental microanalysis and spectroscopic properties were in accord with the solid-state structure.

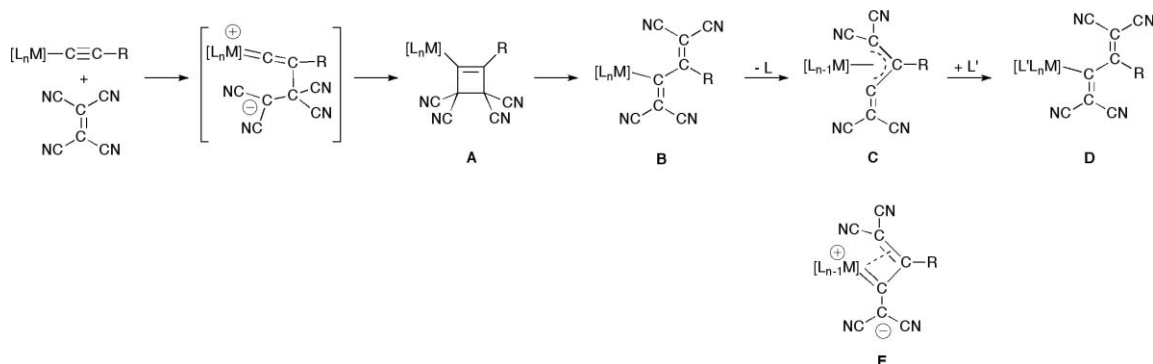
The IR spectrum of **2** contained $\nu(\text{CN})$ bands at 2203 and 2226 cm^{-1} , accompanied by several weak to medium intensity absorptions between 1520 and 1733 cm^{-1} . The ^1H NMR spectrum contained resonances at δ 3.62 (OMe), 4.46 (Cp), 6.53 (NH) and between 6.67 and 7.53 (Ph), while the ^{31}P NMR spectrum contains a singlet at δ 46.9. The extremely low solubility of **2** rendered attempts to obtain the ^{13}C NMR spectrum fruitless. In the electrospray mass spectrum (ES-MS) from a solution containing NaOMe , an ion at m/z 713 is assigned to $[\text{M} + \text{Na}]^+$.

^aSchool of Chemistry & Physics, University of Adelaide, Adelaide, South Australia, 5005. E-mail: michael.bruce@adelaide.edu.au; Fax: + 61 8 8303 4358

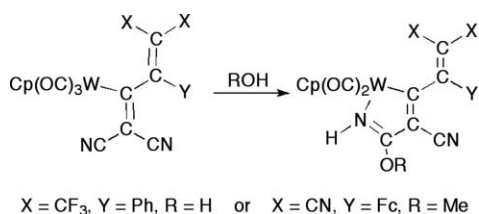
^bDepartment of Chemistry, Durham University, South Road, Durham, UK DH1 3LE

^cChemistry M313, School of Biomedical, Biomolecular and Chemical Sciences, University of Western Australia, Crawley, Western Australia, 6009

† CCDC reference numbers 730741–730749. For crystallographic data in CIF or other electronic format see DOI: 10.1039/b921324d



Scheme 1 The reaction of tene with an alkynyl metal complex to afford a [2 + 2]-cycloadduct, and subsequent transformations.

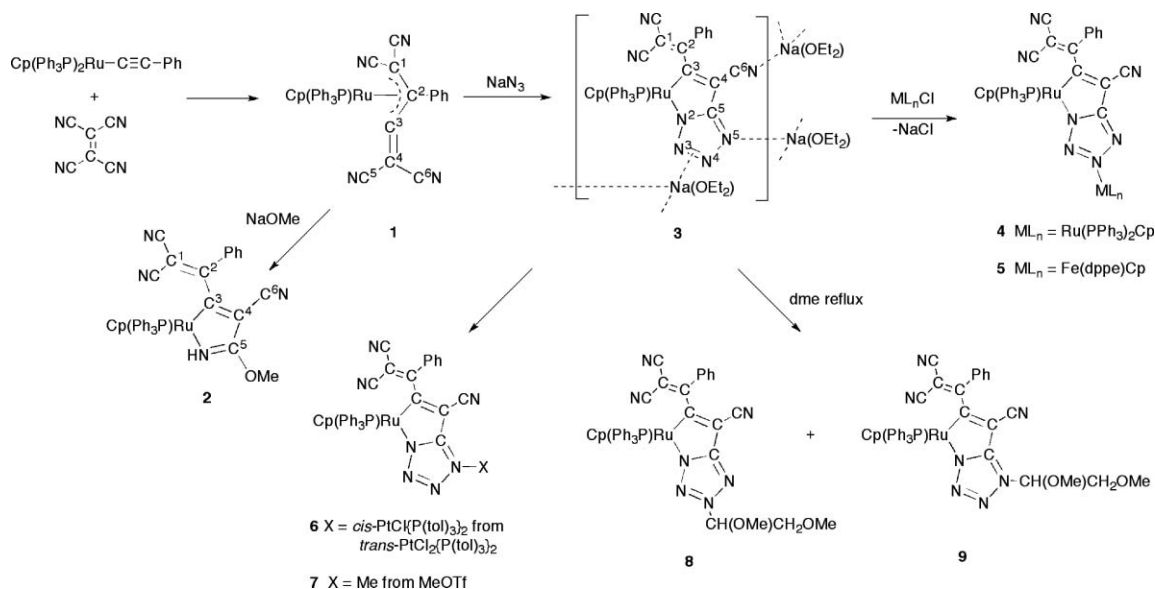


Scheme 2 The hydrolysis and methanolysis of a CN group in W complexes of type **B**.

The “click” reaction^{24,25} between **1** and NaN₃ was carried out in refluxing 1,2-dimethoxyethane (dme) for 24 h, a dark red-purple colour developing over this period. Preparative t.l.c. enabled the separation of the bicyclic tetrazolate as the sodium salt Ru{N₄CC(CN)CCPh=C(CN)₂}(PPh₃)Cp **3** in 88% yield. Spectroscopic data are consistent with the solid-state structure, with ν(CN) bands at 2194 and 2220 cm⁻¹ in the IR spectrum, and resonances for the Cp [δ_{H} 4.33, δ_{C} 79.8 (d, $J(\text{CP}) = 2$ Hz)] and Ph groups (δ_{H} 7.09–7.50, δ_{C} 127.9–134.0) being accompanied by signals for the coordinated Et₂O. The CN groups gave three resonances (δ_{C} 115.6–116.7) and various signals found at δ_{C} 72.3, 100.1, 168.3, 188.5 and 221.0 [d, $J(\text{CP}) = 11$ Hz]

were assigned to the five C(1–5) atoms in the bicyclic ligand. In the ES-MS, ions at m/z 724 and 746 correspond to [anion + (H + Na)]⁺ and [anion + 2Na]⁺, respectively, where the anion is [Ru{N₄CC(CN)CCPh=C(CN)₂}(PPh₃)Cp]⁻. In the negative-ion mode, the ion at m/z 700 corresponds to [M – Na(OEt₂)]⁻.

A minor product from the reaction affording **3** was crystallographically identified as the binuclear complex Ru{N₂N-[Ru(PPh₃)₂Cp]N=CC(CN)=CCPh=C(CN)₂}(PPh₃)Cp **4**, in which the Na(OEt₂) fragment has been replaced by Ru(PPh₃)₂Cp. This reaction requires migration of PPh₃ from part of the reactant, but the reaction between **3** and RuCl(PPh₃)₂Cp afforded this complex in 91% yield, demonstrating that **3** could be a source of binuclear systems containing the tetrazolate bridging group. Accordingly, similar reactions between **3** and FeCl(dppe)Cp and *trans*-PtCl₂{P(tol)₃}₂ afforded the heterometallic compounds Ru{N₂N[Fe(dppe)Cp]N=CC(CN)=CCPh=C(CN)₂}(PPh₃)Cp **5** (76%) and Ru{N₃N[*cis*-PtCl{P(tol)₃}₂]N=CC(CN)=CCPh=C(CN)₂}(PPh₃)Cp **6** (74%) respectively. Both were characterised by single-crystal X-ray structure determinations and elemental microanalyses. In the IR spectra, there are two ν(CN) bands between 2198 and 2222 cm⁻¹, while the ¹H and ³¹P NMR spectra contain resonances arising from the Cp and tertiary phosphine



Scheme 3 The formation of **1** and subsequent reactions.

ligands. ^{195}Pt satellites were present on the $\text{P}(\text{tol})_3$ signals at δ_{p} 3.98 and 14.3 [$J(\text{PP}) = 19$ Hz, $J(\text{Pt}) = 3322$ Hz], consistent with the *cis* stereochemistry. Again, for solubility reasons, a ^{13}C NMR spectrum could be obtained only for **6** and, in addition to resonances for the Me (δ 21.4), Cp (δ 79.8) and aromatic carbons (δ 125.9–135.2) three CN signals (δ 114.4, 114.9, 116.3) and three carbons of the tetrazolate ligand (δ 71.6, 97.2, 185.9) were present. The ES-MS contained $[\text{M} + \text{H} + \text{Na}]^+$ (for **4**) or $[\text{M} + \text{Na}]^+$ (for **5** and **6**) ion clusters.

Treatment of **3** with MeOTf afforded red $\text{Ru}\{\text{N}_3\text{NMe}=\text{CC}(\text{CN})=\text{CCPh}=\text{C}(\text{CN})_2\}(\text{PPh}_3)\text{Cp}$ **7**, for which the presence of the NMe group was indicated by a ^1H NMR signal at δ_{H} 3.89. In the ES-MS, major ions include $[2\text{M} + \text{Na}]^+$ and $[\text{M} + \text{Na}]^+$ at m/z 1453 and 738, respectively. The molecular structure was confirmed by a single-crystal X-ray structure determination. A related complex was obtained serendipitously from the reaction between **3** and *cis*- $\text{RuCl}_2(\text{dppe})_2$ carried out in dme. The red-brown product was not the expected diruthenium derivative, but identified by an X-ray diffraction study as being formed by alkylation of the N(5) atom by the solvent dme, namely $\text{Ru}\{\text{N}_2\text{N}[\text{CH}(\text{CH}_2\text{OME})(\text{OME})]\text{N}=\text{CC}(\text{CN})=\text{CCPh}=\text{C}(\text{CN})_2\}(\text{PPh}_3)\text{Cp}$ **8**. Identification of this complex was also confirmed by the ES-MS, which contains $[2\text{M} + \text{Na}]^+$, $[\text{M} + \text{Na}]^+$ and M^+ ions at m/z 1603, 812 and 790, respectively. In a separate experiment it was established that prolonged heating of **3** in dme at reflux point, in the absence of any other reagents, resulted in formation of **8** (21%) together with its isomer **9** (12%), the latter also being identified by a single-crystal X-ray structure determination. We did not find any evidence for a tautomeric equilibrium between these two compounds.

Molecular structures

The structures of all complexes **1–9** have been determined by crystallographic methods, single molecules of each being illustrated in Fig. 1–8, significant structural parameters for all new complexes being collected in the caption to Fig. 1 (for **1**) and in Table 1 (2–9).

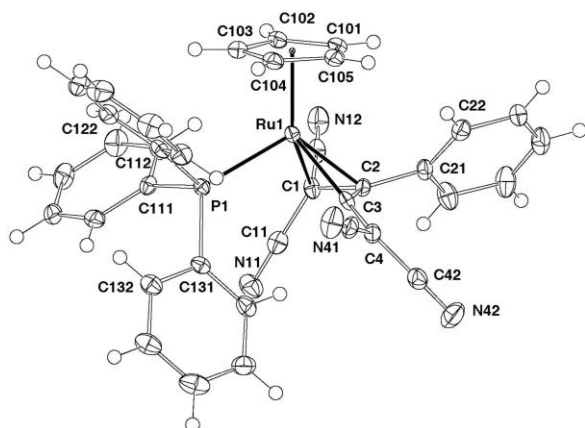


Fig. 1 Plot of a molecule of $\text{Ru}\{\eta^3\text{-C}(\text{CN})_2\text{CPh}=\text{C}(\text{CN})_2\}(\text{PPh}_3)\text{Cp}$ **1**. Bond lengths: Ru(1)–P(1) 2.3734(8), Ru(1)–C(cp) 2.203–2.264(3), av. 2.224, Ru(1)–C(1) 2.182(3), Ru(1)–C(2) 2.130(3), Ru(1)–C(3) 1.979(3), C(1)–C(2) 1.469(4), C(2)–C(3) 1.426(5), C(3)–C(4) 1.354(5) Å. Bond angles: P(1)–Ru(1)–C(1,2) 93.99(9), 115.29(9), P(1)–Ru(1)–C(3) 95.16(9), C(1)–Ru(1)–C(3) 71.4(1), C(1)–C(2)–C(3) 114.4(3), C(2)–C(3)–C(4) 134.8(3)°.

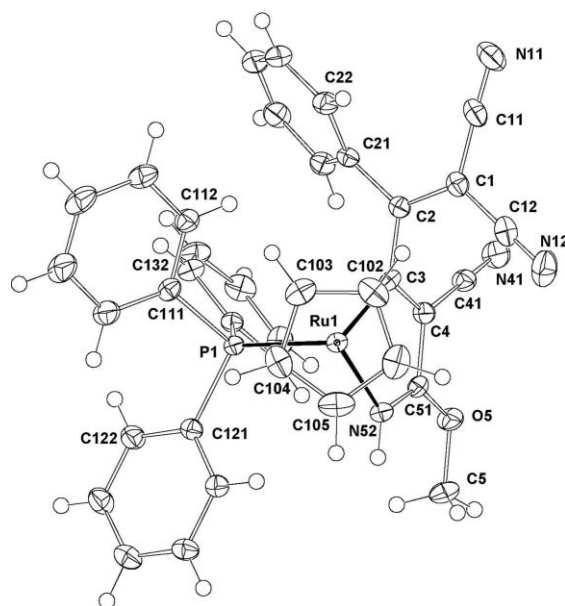


Fig. 2 Plot of a molecule of $\text{Ru}\{\text{NHC}(\text{OMe})\text{C}(\text{CN})=\text{CCPh}=\text{C}(\text{CN})_2\}(\text{PPh}_3)\text{Cp}$ **2**.

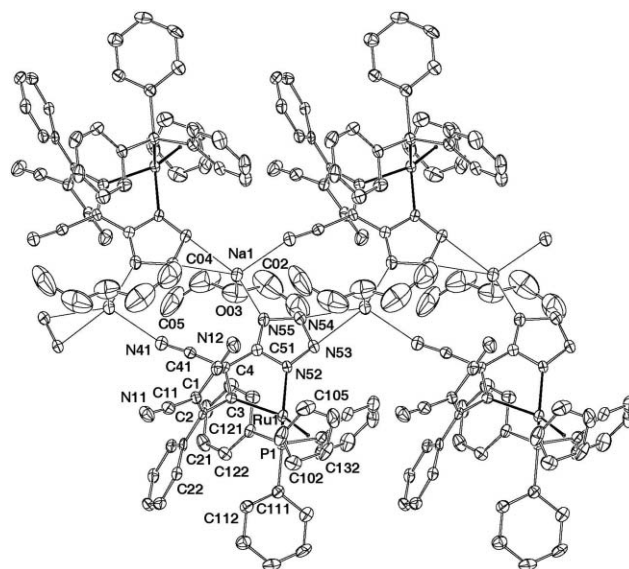


Fig. 3 Plot of a fragment of the polymeric structure of $\text{Ru}\{\text{N}_3\text{N}[\text{Na}(\text{OEt}_2)]\text{C}(\text{CN})=\text{CCPh}=\text{C}(\text{CN})_2\}(\text{PPh}_3)\text{Cp}$ **3**.

The molecular structure of complex $\text{Ru}\{\eta^3\text{-C}(\text{CN})_2\text{CPh}=\text{C}(\text{CN})_2\}(\text{PPh}_3)\text{Cp}$ **1** was reported in our first communication.¹¹ Some disorder was present in the crystal, resulting in less than precise bond parameters being determined, of which the most interesting is the interaction between C(3) and the Ru centre. The Ru–C(3) distance [1.919(5) Å] was found to be shorter than the other two Ru–C separations [2.231, 2.135(4) Å], suggesting some degree of multiple-bond character. The present structure determination of **1** (Fig. 1), from a crystal obtained from MeCN–Et₂O, refined satisfactorily with no signs of anisotropy in C(3) and has yielded bond parameters (see caption to Fig. 1) which are more precise than those obtained in the earlier determination. In particular, the coordination of the Ru centre by the cyanocarbon

Table 1 Selected structural data for complexes **2–9**

Complex	2	3	4	5	6	7	8	9
Bond distances/Å								
Ru(1)–P(1)	2.3152(3)	2.2965(8)	2.3127(6)	2.301(2)	2.306(2)	2.3262(6)	2.3242(5)	2.3211(5)
Ru(1)–C(cp)	2.189–2.245(1)	2.191–2.224(4)	2.176–2.231(2)	2.155–2.185(12)	2.184–2.227(9)	2.208–2.239(2)	2.194–2.226(2)	2.195–2.247(2)
(av.)	2.215	2.208	2.200	2.170	2.207	2.221	2.210	2.218
Ru(1)–C(3)	2.043(1)	2.047(3)	2.050(2)	2.055(9)	2.038(7)	2.035(2)	2.052(2)	2.033(2)
Ru(1)–N(52)	2.106(1)	2.076(3)	2.095(2)	2.057(8)	2.059(7)	2.082(2)	2.057(2)	2.057(2)
C(1)–C(2)	1.370(2)	1.379(5)	1.364(3)	1.39(1)	1.36(1)	1.361(2)	1.364(3)	1.362(3)
C(2)–C(3)	1.457(2)	1.464(4)	1.462(3)	1.46(1)	1.48(1)	1.470(3)	1.466(3)	1.463(3)
C(3)–C(4)	1.377(2)	1.369(5)	1.366(3)	1.36(1)	1.36(1)	1.376(3)	1.370(3)	1.392(2)
C(4)–C(51)	1.441(2)	1.442(4)	1.450(3)	1.43(1)	1.44(1)	1.436(3)	1.436(3)	1.437(2)
C(51)–N(52)	1.295(2)	1.348(4)	1.345(2)	1.35(1)	1.352(9)	1.335(3)	1.364(3)	1.337(2)
C(51)–N(55)		1.331(4)	1.330(3)	1.33(1)	1.32(1)	1.341(3)	1.320(3)	1.348(2)
N(52)–N(53)		1.346(4)	1.341(2)	1.33(1)	1.351(9)	1.363(2)	1.326(2)	1.366(2)
N(53)–N(54)		1.309(4)	1.330(2)	1.33(1)	1.323(9)	1.300(3)	1.318(3)	1.290(2)
N(54)–N(55)		1.365(4)	1.350(2)	1.37(1)	1.347(8)	1.360(3)	1.336(3)	1.366(2)
C(1)–C(11,12)	1.439, 1.432(2)	1.441, 1.431(5)	1.445, 1.447(3)	1.43, 1.42(2)	1.47, 1.45(1)	1.448, 1.441(3)	1.443, 1.439(3)	1.445, 1.435(3)
C(2)–C(21)	1.486(2)	1.482(5)	1.483(3)	1.49(2)	1.48(1)	1.491(3)	1.485(3)	1.485(3)
C(4)–C(41)	1.432(2)	1.435(5)	1.432(3)	1.42(2)	1.46(1)	1.437(3)	1.437(3)	1.431(3)
Bond angles/°								
P(1)–Ru(1)–C(3)	97.98(3)	95.49(9)	97.71(6)	96.7(3)	95.9(2)	94.87(6)	97.85(5)	94.87(5)
P(1)–Ru(1)–N(52)	91.28(3)	90.84(8)	86.98(5)	90.1(2)	80.9(2)	86.78(5)	87.74(5)	89.73(5)
C(3)–Ru(1)–N(52)	76.82(4)	75.8(1)	76.41(7)	75.7(3)	76.2(3)	76.27(8)	76.52(7)	76.48(7)
Ru(1)–C(3)–C(2)	124.75(8)	122.5(2)	121.6(2)	119.2(7)	121.2(6)	122.6(2)	120.7(1)	121.5(1)
Ru(1)–C(3)–C(4)	116.08(8)	118.1(2)	118.4(2)	118.4(7)	118.7(6)	118.6(2)	118.0(1)	118.0(1)
Ru(1)–N(52)–C(51)	116.74(8)	118.1(2)	116.6(1)	117.9(7)	117.5(5)	116.7(2)	117.7(1)	117.5(1)
Ru(1)–N(52)–N(53)		135.9(2)	136.4(1)	135.8(6)	135.7(5)	136.1(2)	135.0(1)	134.8(1)
C(1)–C(2)–C(3)	119.0(1)	116.7(3)	120.6(2)	119.4(1)	121.2(6)	120.8(2)	121.2(2)	119.2(2)
C(2)–C(3)–C(4)	118.8(1)	118.8(3)	119.4(2)	122.1(9)	119.5(7)	118.6(2)	120.7(2)	119.7(2)
C(3)–C(4)–C(51)	114.8(1)	113.8(3)	113.3(2)	113.4(9)	112.8(7)	112.4(2)	113.6(2)	112.0(2)
C(4)–C(51)–N(52)	115.6(1)	113.5(3)	115.2(2)	114.5(9)	114.5(7)	115.8(2)	114.2(2)	115.3(2)
C(4)–C(51)–N(55)			133.0(2)	133.6(9)	136.9(7)	136.7(2)	134.2(2)	137.6(2)
C(51)–N(52)–N(53)		105.9(3)	106.9(2)	105.7(8)	106.8(6)	107.0(2)	107.3(2)	107.6(2)
C(51)–N(55)–N(54)		104.0(3)	103.0(2)	104.1(7)	107.9(6)	108.6(2)		108.3(2)
N(52)–N(53)–N(54)		108.2(3)	106.0(2)	108.8(8)	108.3(6)	109.8(2)	104.4(2)	109.45(2)
N(53)–N(54)–N(55)		110.7(3)	112.4(2)	109.7(8)	108.3(6)	107.0(2)	115.2(2)	107.6(2)
N(52)–C(51)–N(55)		111.3(3)	111.7(2)	111.7(9)	108.5(7)	107.6(2)	111.5(2)	107.0(2)

For **2**: C(51)–O(5) 1.336(1), C(5)–O(5) 1.433(2) Å; C(4)–C(51)–O(5) 115.9(1), C(5)–O(5)–C(51) 118.5(1)°. For **3**: Na(1)–N(41') 2.403(3), Na(1)–N(53'') 2.427(3), Na(1)–N(54'') 2.585(3), Na(1)–N(55) 2.367(3), Na(1)–O(03) 2.438(4) Å; N(41')–Na(1)–N(53'') 108.6(1), N(41')–N(1)–N(54'') 134.7(1), N(41')–Na(1)–N(55) 94.2(1), N(41')–Na(1)–O(03) 98.1(1), N(53'')–Na(1)–N(54'') 30.07(9), N(53'')–Na(1)–N(55) 137.7(1), N(53'')–Na(1)–O(03) 102.1(1), N(54'')–Na(1)–N(55) 111.4(1), N(54'')–Na(1)–O(03) 106.9(1), N(55)–Na(1)–O(03) 109.5(1)°, where ' and '' refer to the atoms at $-x, 1/2 + y, 1/2 - z$ and $-x, y - 1/2, 1/2 - z$, respectively. For **4**: Ru(2)–P(2,3) 2.3393(6), 2.3228(6), Ru(2)–C(cp) 2.216–2.231(2), (av.) 2.220, Ru(2)–N(54) 2.085(2) Å; P(2)–Ru(2)–P(3) 99.63(2), P(2,3)–Ru(2)–N(54) 92.33(5), 88.35(5), Ru(2)–N(54)–N(55, 55) 121.7(1), 125.9(1)°. For **5**: Fe(2)–P(2,3) 2.220(4), 2.187(3), Fe(2)–C(cp) 2.06–2.11(1), (av.) 2.08, Fe(2)–N(54) 2.008(9) Å; P(2)–Fe(2)–P(3) 83.6(1), P(2, 3)–Fe(2)–N(54) 92.2(2), 95.1(3), Fe(2)–N(54)–N(53, 55) 124.0(7), 125.2(6)°. For **6**: Pt(1)–Cl(1) 2.336(2), Pt(1)–N(55) 2.058(6), Pt(1)–P(2, 3) 2.254(2), 2.268(2) Å; Cl(1)–Pt(1)–N(55) 87.3(2), Cl(1)–Pt(1)–P(2, 3) 86.61(7), 175.68(8), N(55)–Pt(1)–P(2, 3) 89.9(2), 172.5(2), P(2)–Pt(1)–P(3) 96.47(7), Pt(1)–N(55)–C(51) 133.3(5), Pt(1)–N(55)–N(54) 118.2(5)°. For **7**: N(55)–C(55) 1.465(3) Å; C(51)–N(55)–C(55) 130.6(2), C(51)–N(55)–N(54) 108.6(2), C(55)–N(55)–N(54) 120.8(2)°. For **8**: C(03)–N(54) 1.503(3), C(03)–O(02) 1.326(4), C(03)–C(04) 1.532(4), C(01)–O(02) 1.429(5), C(04)–O(05) 1.377(3), C(06)–O(05) 1.439(4) Å; C(03)–N(54)–N(53, 55) 121.4(2), 122.1(2), N(54)–C(03)–O(02) 111.3(3), N(54)–C(03)–C(04) 109.8(2), C(01)–O(02)–C(03) 115.1(3), C(03)–C(04)–O(05) 107.0(2), C(04)–O(05)–C(06) 112.1(2), N(52)–C(51)–C(4) 114.2(2), O(02)–C(03)–C(04) 112.9(2)°. For **9**: C(03)–N(55) 1.481(2), C(03)–O(02) 1.383(3), C(03)–C(04) 1.539(3), C(01)–O(02) 1.432(3), C(04)–O(05) 1.425(3), C(06)–O(05) 1.417(3) Å; C(03)–N(55)–N(54) 119.3(2), N(55)–C(03)–O(02) 111.7(2), N(55)–C(03)–C(04) 107.4(2), C(01)–O(02)–C(03) 113.4(2), C(03)–C(04)–O(05) 107.3(2), C(04)–O(05)–C(06) 114.6(2), N(52)–C(51)–C(4) 115.2(2), O(02)–C(03)–C(04) 109.1(2)°.

ligand is more accurately determined. The presently determined values for Ru–C(1, 2, 3) are 2.182(3), 2.130(3), 1.979(3) Å, respectively. These values are similar to those reported for the Cp* analogue of **1**.¹³ Along the C₄ chain, C–C separations are 1.469(4), 1.426(5) and 1.354(5) Å for C(1)–C(2), C(2)–C(3) and C(3)–C(4) bonds, respectively. The C(1)–C(2) and C(2)–C(3) separations [1.469(4), 1.426(5) Å, respectively] are consistent with an allylic group coordinated to a metal. The C(3)–C(4) separation [1.354(5) Å] resembles those found for other cyano-olefins. The Ru–P(1) [2.3734(8) Å] and Ru–C(cp) distances [2.203–2.264(3), av. 2.224 Å] fall within the usual ranges found for related Ru(PPh₃)Cp complexes.

Common features of the structures of **2–9** include the Ru(PPh₃)Cp group chelated by a C₃N fragment which carries the 1,1-dicyano-2-phenylvinyl substituent on C(3) that forms part of the η³-dienyl ligand present in **1**, now displaced by N(5) of the new ligand. The ruthenium atom is pseudo-octahedrally coordinated by the Cp [Ru–C(cp) (av.) 2.17–2.22 Å] and PPh₃ ligands [Ru–P 2.2965(8)–2.3262(6) Å] and C(3) and N(5) of the chelating ligand [Ru–C(3) 2.033(2)–2.055(9), Ru–N(52) 2.057(2)–2.106(1) Å]. Around the RuC₃N ring, C(3)–C(4) and C(4)–C(51) [1.36(1)–1.392(2), 1.43(1)–1.450(3) Å, respectively] are consistent with their being C=C double and C–C single bonds, while in **3–8** C(51)–N(52) [1.345(2)–1.364(3) Å] has double bond character.

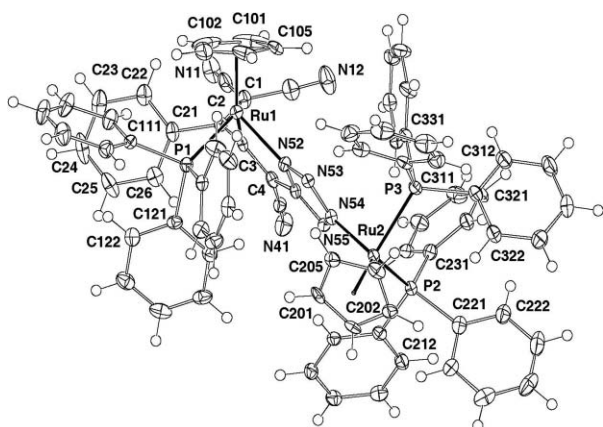


Fig. 4 Plot of a molecule of $\text{Ru}\{\text{N}_2\text{N}[\text{Ru}(\text{PPh}_3)_2\text{Cp}]\text{N}=\text{CC}(\text{CN})=\text{CCPh}=\text{C}(\text{CN})_2\}(\text{PPh}_3)\text{Cp}$ **4**.

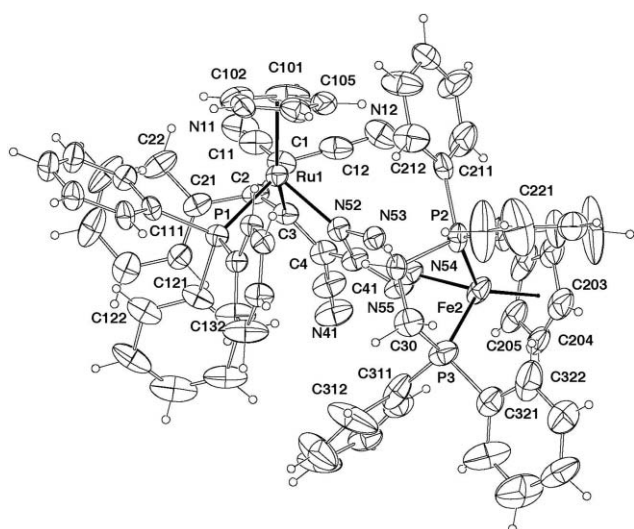


Fig. 5 Plot of a molecule of $\text{Ru}\{\text{N}_2\text{N}[\text{Fe}(\text{dppe})\text{Cp}]\text{N}=\text{CC}(\text{CN})=\text{CCPh}=\text{C}(\text{CN})_2\}(\text{PPh}_3)\text{Cp}$ **5**.

Within the $\text{CPh}=\text{C}(\text{CN})_2$ fragment, there are no unusual features requiring comment, while the OMe substituent in **2** [$\text{C}(51)\text{--O}(51)$ 1.433(2) Å] is also conventional.

Cycloaddition of azide to $\text{CN}(5)$ in **1** has given the tetrazolato group in **3–9** which comprises atoms $\text{C}(51)\text{N}(52\text{--}55)$, attached to Ru by $\text{N}(52)$ [2.057(2)–2.095(2) Å]. Around the ring, $\text{C}(51)\text{--N}(55)$ ranges between 1.320(3) and 1.348(2) Å, while the N--N distances range between 1.290(2) and 1.366(2) Å. Shorter $\text{N}(53)\text{--N}(54)$ distances are found for **3**, **7** and **8** [1.300(3)–1.318(3) Å]. In **3**, the $[\text{Na}(\text{OEt}_2)]^+$ cation is attached to the complex anion *via* coordination to $\text{N}(55)$ and also to $\text{N}(53, 54)$ and $\text{N}(41)$ from two other anions related by crystallographic 2_1 screw axes. The separation $\text{N}(53)\text{--N}(54)$ [1.309(4) Å] corresponds to an $\text{N}=\text{N}$ double bond, so that the $\text{Na--N}=\text{N}$ interaction is properly described as a π bond, similar to those found in related pyrazolate salts containing Group 11 or 12 metal cations.^{26,27}

Replacement of the $\text{Na}(\text{OEt}_2)$ cation by transition metal fragments $\text{Ru}(\text{PPh}_3)_2\text{Cp}$ (in **4**), $\text{Fe}(\text{dppe})\text{Cp}$ (in **5**) or *cis*- $\text{PtCl}\{\text{P}(\text{tol})_3\}_2$ (in **6**) results in the Group 8 metals being attached to $\text{N}(54)$ [$\text{Ru--N}(54)$ 2.085(2), $\text{Fe--N}(54)$ 2.008(9) Å] while Pt is bonded to $\text{N}(55)$ [2.058(6) Å]. The usual pseudo-octahedral geometries are found

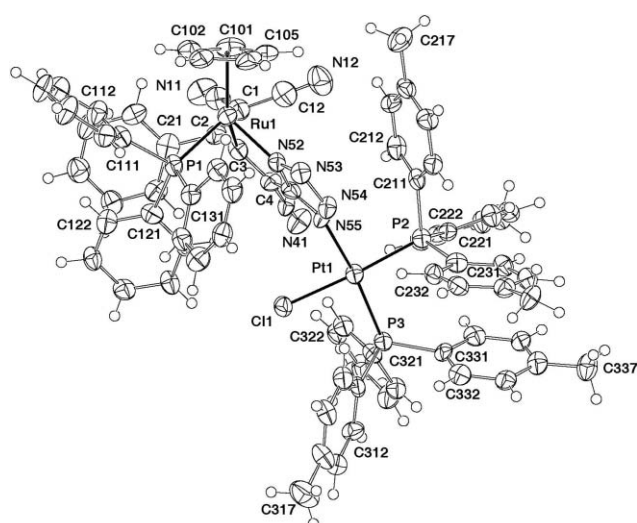


Fig. 6 Plot of a molecule of $\text{Ru}\{\text{N}_3\text{N}[\text{PtCl}\{\text{P}(\text{tol})_3\}_2\text{-cis}]=\text{CC}(\text{CN})=\text{CCPh}=\text{C}(\text{CN})_2\}(\text{PPh}_3)\text{Cp}$ **6**.

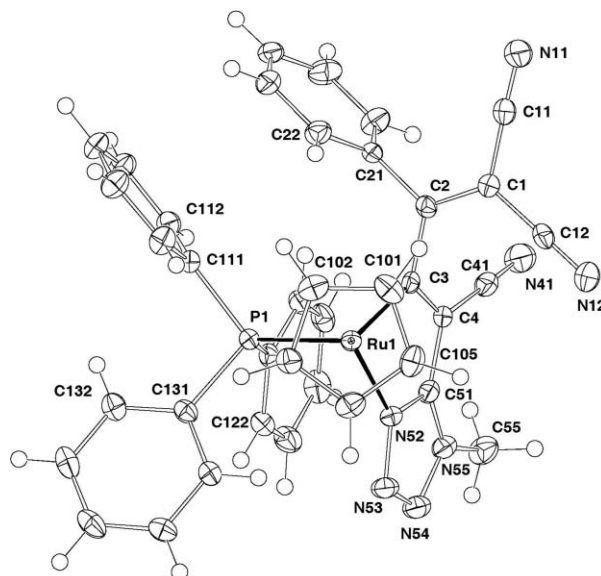


Fig. 7 Plot of a molecule of $\text{Ru}\{\text{N}_3\text{NMe}=\text{CC}(\text{CN})=\text{CCPh}=\text{C}(\text{CN})_2\}(\text{PPh}_3)\text{Cp}$ **7**.

for the Fe and Ru fragments, while the Pt centre is distorted square-planar [$\text{P}(2)\text{--Pt--P}(3)$ 96.47(7)°, other angles at Pt 86.61(7)–89.8(2)°], with the larger angle at Pt caused by steric repulsion between the two large mutually *cis* $\text{P}(\text{tol})_3$ ligands.

Similar disparity in sites of attachment is found for **7–9**, where the Me group in **7** is bonded to $\text{N}(55)$, whereas the dme-derived groups in **8** and **9** are attached to $\text{N}(54)$ and $\text{N}(55)$, respectively. The C--C , C--O and C--N bond parameters have no unusual features, the different sites of attachment resulting in localisation of the $\text{C}=\text{N}$ and $\text{N}=\text{N}$ double bonds.

Computations

Molecular structures determined for several transition metal complexes containing the η^3 -tetracyanobutadienyl ligand such as **1** all show that the $\text{M--C}(3)$ bond is substantially shorter than the

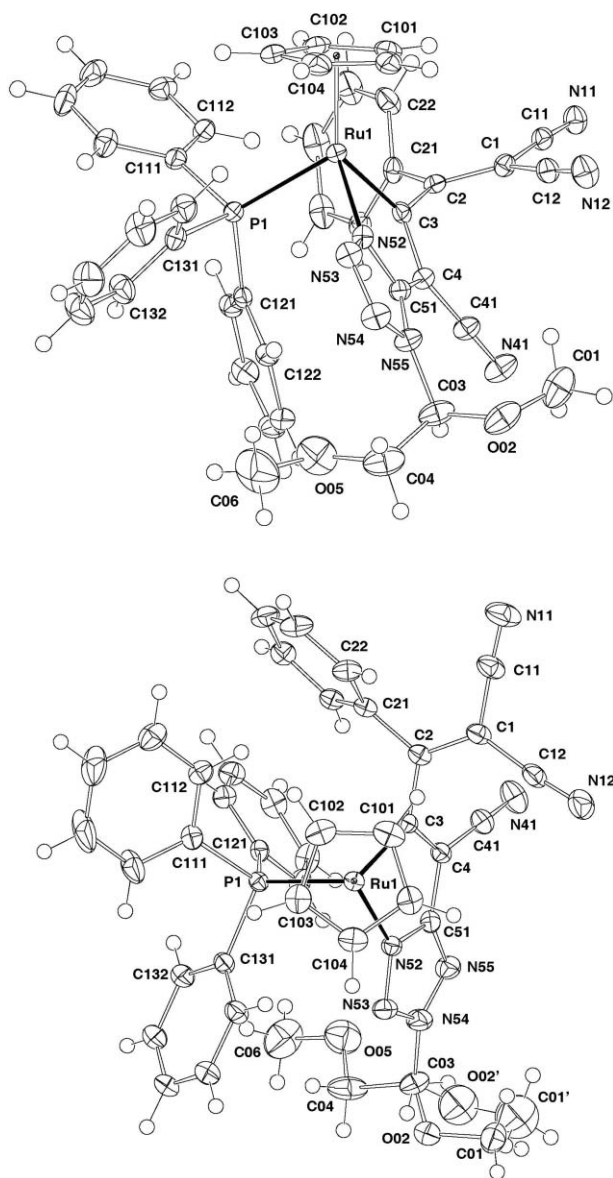


Fig. 8 Plots of molecules of $\text{Ru}\{\text{N}_2\text{N}[\text{CH}(\text{CH}_2\text{OMe})(\text{OMe})]\text{N}=\text{CC}(\text{CN})=\text{CCPh}=\text{C}(\text{CN})_2\}\text{(PPh}_3\text{)Cp}$ **8** (lower) and $\text{Ru}\{\text{N}_3\text{N}[\text{CH}(\text{CH}_2\text{OMe})(\text{OMe})]=\text{CC}(\text{CN})=\text{CCPh}=\text{C}(\text{CN})_2\}\text{(PPh}_3\text{)Cp}$ **9** (upper).

M–C(2) and M–C(1) bonds whereas the C(1)–C(2) and C(2)–C(3) bonds are nearly equivalent.^{2,6,9,12–14} These characteristics are also evident in experimental structures of related η^3 -cyanobutadienyl ligands.^{16,17,19} Indeed, crystallographically determined structures of complexes with η^3 -butadienyl ligands generally show a trend for the M–C(3) bond to be shorter than the M–C(2) and M–C(1) bonds. This contraction becomes quite obvious in cases where strong electron-withdrawing groups such as CN and CF_3 are present at C(4) and is accompanied by elongation of the C(3)–C(4) bond.²⁸ This pattern of bond lengths is often interpreted as evidence for contribution to the structure of these compounds from a zwitterionic form **E** (Scheme 1),^{9,13,16,29–32} noting that the orientation of the substituents at C(4) rules out π -conjugation between C(4) and the allyl π -orbitals.^{29,32}

In order to understand the bonding and reactivity patterns in complexes containing the η^3 -cyanobutadienyl ligand, Wiberg

bond orders and natural charges have been computed on the X-ray geometry of **1** and these are summarised in Fig. 9. Good quality data for the X-ray geometry of an η^3 -allyl complex $\text{Ru}\{\eta^3\text{-CH}_2\text{CMeCHC}(\text{O})\text{Me}\}\text{(PPh}_3\text{)Cp}^*$ **10** are also included for comparison.³³ Most notably, the nucleophilic attack at the carbon atom C(5) in **1** by the methoxide anion is consistent with the highest positive charge of 0.29 calculated on C(5) of the butadienyl ligand. The azide anion appears to attack selectively one of four CN groups present in **1** to form the anion found in **3**. It is likely that the most polar CN group, at CN(5), as shown by calculated charges, is preferred for the dipolar [3 + 2] cycloaddition process.

The bond order of 0.68 for Ru–C(3) in the η^3 -butadienyl complex **1** is almost double that found in the η^3 -allyl complex **10** (0.36) although the charges at Ru are comparable (**1**, +0.49; **10**, +0.45). The C(3)–C(4) bond order of 1.57 in **1** is somewhat less than expected for a double bond and the substantial negative charge of –0.34 at C(4) supports the description of complexes containing the η^3 -tetracyanobutadienyl ligand as intermediate between **C** and the zwitterion geometry **E** (Scheme 1). Natural bond orbital (NBO) analysis of the orbitals involved in the bonding of **1** reveals that both the sp^2 and p orbitals at C(3) (19% s, 81% p) are involved in the Ru–C(3) bond, whereas only the π -orbitals of C(1)=C(2) (5% s, 95% p) contribute to the Ru–C(1) and Ru–C(2) bonds respectively.

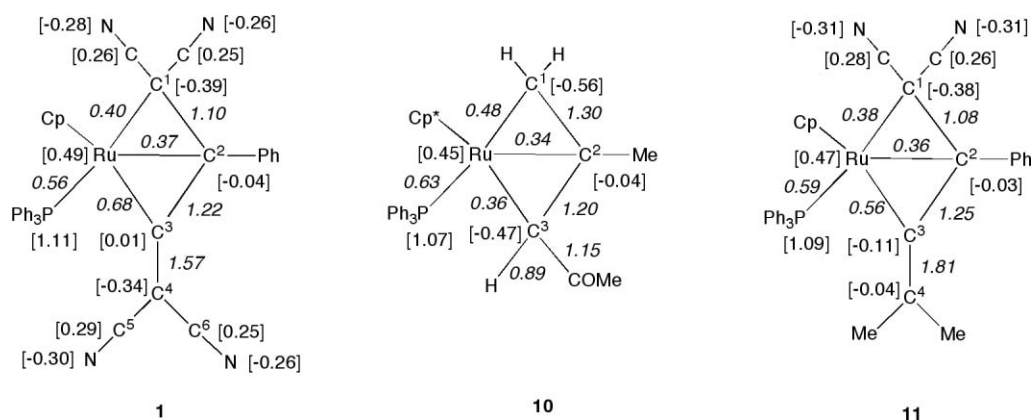
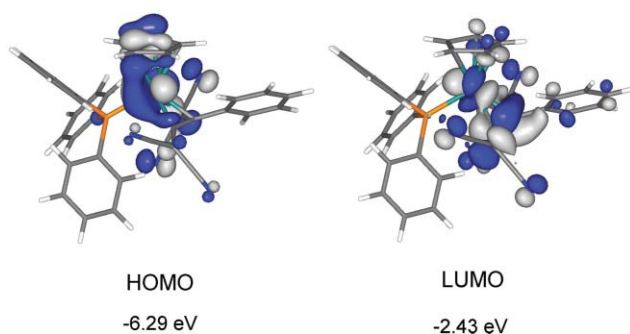
The Ru–C(3) bond length depends on the substituents at C(4). For example, the contraction of the Ru–C(3) bond length relative to the Ru–C(1) and Ru–C(2) bonds is not so obvious in structures of ruthenium η^3 -butadienyl complexes with less strongly electron-withdrawing groups.^{30,34,35} Since ruthenium complexes with electron-donating substituents at C(4) are not known experimentally, the DFT-optimised geometry of the model compound **11** derived from compound **1** by substitution of the CN moieties at C(4) by methyl groups was calculated. The Ru–C(3) bond in **11** is elongated by 0.1 Å compared to **1**, with little change in the Ru–C(1) and Ru–C(2) bond lengths. Nevertheless, the Ru–C(3) bond is still shorter than the other two Ru–C bonds by 0.05–0.10 Å. Natural bond order (NBO) analysis of the orbitals in the bonding of **11** reveals very similar compositions to those of the analogous orbitals in **1**. It therefore appears that the “short” M–C(3) bond length is a general feature for all neutral transition metal η^3 -butadienyl complexes.^{29,31,32,36}

Whilst the charges on the metal for the optimised geometries of **1** and **11** are essentially identical (+0.49 and +0.47, respectively), greater variation is found in the charges on the C(3) and C(4) atoms (Fig. 9). The changes in calculated bond order in **1** compared to **11** are chemically sensible and clearly support the notion that the electron-withdrawing groups at C(4) stabilise the zwitterionic form **E**.

Molecular orbital (MO) calculations on **1** showed the LUMO to be mainly on the metal- η^3 -tetracyanobutadienyl moiety whereas the HOMO is located on the metal and the Cp ring (Fig. 10, Table 2). MO calculations on the optimised geometry of **11** reveal similar frontier orbitals but the HOMO and LUMO energies are 0.74 and 0.97 eV higher in energy when compared to **1**. Computed MO data obtained from the η^3 -allyl complex **10** show the HOMO to be similar to those found for **1** and **11** but the LUMO is located on the PPh_3 moiety rather than on the η^3 -allyl ligand. The low LUMO and HOMO energies in **1** are in agreement with the oxidation and reduction waves observed elsewhere for derivatives

Table 2 Molecular orbital energies and compositions for **1**, **10** and **11**

1		eV	Ru	Cp	PPh ₃	C(1)	C(2)	C(3)	(CN) ₂	Ph	C(CN) ₂
169	L + 1	-1.88	44	25	21	0	1	0	3	2	2
168	LUMO	-2.43	22	8	3	17	14	13	7	8	8
167	HOMO	-6.29	44	22	6	5	0	3	9	0	10
166	H - 1	-6.38	20	13	16	20	5	2	1	22	1
10		eV	Ru	Cp*	PPh ₃	C(1)	C(2)	C(3)	H ₂	Me	CO ₂ MeH
157	L + 1	-0.45	10	5	79	1	0	1	0	0	4
156	LUMO	-0.64	3	3	94	0	0	0	0	0	0
155	HOMO	-4.65	43	27	9	6	0	9	0	0	5
154	H - 1	-4.95	80	8	2	2	3	1	0	0	4
11		eV	Ru	Cp	PPh ₃	C(1)	C(2)	C(3)	(CN) ₂	Ph	CMe ₂
165	L + 1	-1.30	39	21	32	1	1	0	2	3	0
164	LUMO	-1.46	27	10	4	9	15	1	11	17	4
163	HOMO	-5.55	46	14	7	7	0	7	6	0	12
162	H - 1	-5.71	27	15	8	4	3	10	3	12	18

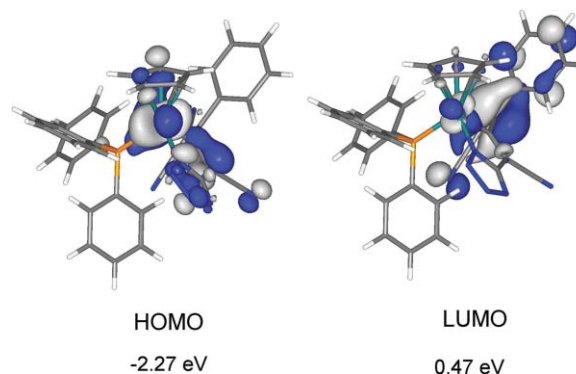
**Fig. 9** Wiberg bond indices (italics) and natural charges (square brackets) for **1**, **10** and **11**.**Fig. 10** Frontier orbitals for **1**. Contour values are plotted at ± 0.04 (e/bohr^3)^{1/2}.

related to **1**.⁶ The reductions of **1** and related derivatives are likely to take place at the metal- η^3 -tetracyanobutadienyl moieties.

The anion in **3** was shown to react with electrophiles to form compounds with substituents at one of two nitrogen atoms of the tetrazolato ring, N(4) or N(5). Comparison between the optimised and experimental geometries for the anion in **3** reveals little differences in the tetrazolato cycle despite the Na \cdots N interactions between the anion and cation found in the solid state geometry.

This suggests that the Na \cdots N interactions are weak and the anion in **3** is likely to be discrete in solution.

Fig. 11 shows the frontier orbitals for the anion in **3** where the HOMO involves the Ru atom and the N₄C ring and the HOMO energy is relatively high as expected for an anion. The LUMO in the anion of **3** is mainly the π^* orbital on the C=C double bond of the CPh=C(CN)₂ group. Charge calculations on both

**Fig. 11** Frontier orbitals for anion in **3**. Contour values are plotted at ± 0.04 (e/bohr^3)^{1/2}.

optimised and experimental geometries of the anion show the N(5) atom to have the highest negative charge (−0.33) of the three unsaturated nitrogen atoms [−0.13 for N(4) and −0.15 for N(3)] in the N₄C ring. This is in accord with formation of the 5-substituted products **6** and **7** from the reactions of **3** with *trans*-PtCl₂{P(tol)₃}₂ and MeOTf, respectively.

In contrast, the formation of the 4-substituted products, **4** and **5**, rather than the 5-substituted analogues may be attributed to the steric effects of the electrophiles [Ru(PPh₃)₂Cp]⁺ and [Fe(dppe)Cp]⁺, which prevent formation of M–N bonds with the more negative N(5) and N(3) atoms. Optimisations of two geometries of **5** where the Fe(dppe)Cp fragment is at the 4- or 5-position revealed the 4-substituted isomer to be more stable than the 5-substituted isomer by 5.6 kcal mol^{−1}. The steric effect of the Fe(dppe)Cp fragment is obvious in the 5-substituted isomer where the Fe–N–N angle is 109.6° whereas in the 4-substituted isomer the Fe–N–N angle is 122.9° suggesting little steric effect in the latter. The latter value is close to the angle of 125.2(6)° observed experimentally for **5**. The formation of both 4- and 5-substituted products **8** and **9** in low yields from **3** in refluxing dme is likely to be a radical process rather than an electrophilic process where only product **9** would be expected. According to the energies of the optimised geometries for products **8** and **9**, the 5-substituted isomer **9** is 6.9 kcal mol^{−1} more stable than isomer **8**.

NMR spectra

The ¹³C NMR shifts for the butadienyl carbons in **1** were tentatively assigned in the earlier study.³ The order of the resonances on going from low to high field was assigned to C(3), C(1), C(4) and C(2). This contrasts with the order of resonances at C(3), C(4), C(2) and C(1) found for other neutral transition metal η³-butadienyl complexes in more recent literature.^{36–40} Calculated NMR shifts obtained from the geometry of **1** reveal the order to be C(3), C(4), C(2) and C(1) and thus the experimental ¹³C NMR data for **1** are reassigned here (see Experimental). Calculated ¹³C NMR shifts for the anion in **3** and for the platinum complex **6** were also used to aid assignments of their experimental ¹³C data. The optimised geometry for a model of **6**, in which the tolyl groups have been substituted by phenyl rings, features a large P–Pt–P angle (98.5°) which is in accord with the experimental geometry [96.47(7)°].

Discussion

Ligand displacement reactions of complexes containing η³-tetracyanobutadienyl ligands are reported to form complexes containing η¹-tetracyanobutadienyl ligands, suggesting that the Ru–C(3) bond is stronger than the Ru–(η²-C=C) attachment.^{3,11} Similarly, attack on one of the CN groups by nucleophiles to generate amido groups may give chelating ligands with concomitant displacement of the coordinated dicyanovinyl group, as observed previously with tungsten complexes (Scheme 2).^{7,15}

In the present study, the reaction between **1** and NaOMe affords complex **2** containing a methoxy(amido) ligand, the η²-CPh=C(CN)₂ group being displaced from the Ru centre. The methoxide acts as a nucleophile attacking at C(5), which is the most positively charged carbon based on computed charges on the geometry of **1**. The resulting C(OMe)N[−] group interacts with

the Ru centre and is converted to **2** during work-up. Protonation of the nitrogen by MeOH solvent occurring concomitantly with addition of OMe at the carbon atom cannot, however, be ruled out. Structural parameters of **2** are similar to those of the related tungsten complexes mentioned above.^{7,15}

Current interest in “click chemistry” encouraged us to examine the reaction between **1** and sodium azide.^{24,25} There is precedent in the “reverse” reaction between Ru(N₃)(PP)Cp and nitriles or isonitriles, which afforded the tetrazolato complexes Ru(N₄C)(PP)Cp.^{40–43} The product from the reaction of **1** with NaN₃ was determined to be the sodium salt of the anionic tetrazolate **3**, in which each Na⁺ cation interacts with three anions to give a polymeric array. The bicyclic ligand incorporates the Ru centre, with a Na(OEt₂) fragment interacting with two nitrogen atoms of one molecule [N(53,54)], a third [N(55′)] from a second molecule, and a CN group [N(41′′)] from a third anion, together with an Et₂O molecule (Fig. 3). The interaction between the sodium and N(53)–N(54) is properly described as η² (or κ²).^{26,27} It is likely that a [3 + 2]-cycloaddition of the CN(5) group in **1** to azide anion takes place to form the tetrazolato anion, which then interacts with the Ru centre with conversion to anion **3**.

Reactions between **3** and several metal halide complexes proceed by salt elimination to give the binuclear Ru₂, Ru–Fe and Ru–Pt complexes **4–6**. In **4** and **5**, the M(PP)Cp′ fragment is σ-bonded to N(4), whereas in **6**, the Pt is attached to N(5) (Scheme 3). In **7**, formed by methylation of **3** with MeOTf, the Me group is bonded to N(5). Computations show the N(5) atom to have the highest negative charge of the three unsaturated nitrogen atoms N(3), N(4) and N(5). Thus electrophilic attack would be expected to occur at N(5) as observed in the formation of **6** and **7**. It is likely that the site of attachment N(4) observed for **4** and **5** is a function of the steric demands of the ML_n groups. This assumption is supported by the observed rearrangement of the *trans* to *cis* conformation at the Pt centre to reduce steric effects and to allow Pt–N(55) bond formation in **6** which is not possible for the more bulky Fe and Ru fragments.

The products **8** and **9**, formed in low yields from reactions of **3** with the solvent dme, contain the alkyl group MeOCH₂CH(OMe) attached to either N(4) or N(5). From the low and non-selective yields of products, it is believed that radical rather than electrophilic processes are taking place in these reactions. The two isomers are formed in similar amounts, reflecting the usual lack of site preference found in reactions of pyrazoles and similar five-membered *N*-heterocycles. There is no evidence for any tautomeric equilibrium between **8** and **9**. Compound **9** would be expected to be the sole (or major) isomer in any equilibrium according to the relative stabilities of **8** and **9**.

Conclusions

Complex **1** is obtained in high yield from the reaction between tcne and Ru(C≡CPh)(PPh₃)₂Cp. One of the CN groups in the η³-tetracyanobutadienyl ligand has proved to be susceptible to nucleophilic attack. Reaction of **1** with methoxide has given the methoxy(amido) compound **2**, in which a chelating ligand containing a RuC₃N cycle is present. Addition of azide to a CN group affords the bicyclic anion found in **3** with RuC₃N and N₄C rings, which can be further derivatised with metal–ligand fragments *via* salt-elimination reactions. The dimetallic products

show that electrophilic attack at one of the three unsaturated nitrogen atoms of the N_4C ring takes place selectively and the site of attack depends on the size of the electrophile. Natural charge calculations show that the cyanide group involved in the reactions of **1** with methoxide and azide has a greater positive charge at C and a greater negative charge at N than those calculated for the other three cyanide groups present in **1**. In all of the products, the dicyano(phenyl)vinyl substituent no longer interacts with the Ru centre, in contrast to the situation in precursor **1**. DFT computations show that the short Ru–C(3) bond length compared to Ru–C(1) and Ru–C(2) in **1** largely results from the presence of the strongly electron-withdrawing CN groups at C(4), and contrasts with related complexes containing a η^3 -butadienyl ligand with less electron-withdrawing substituents at C(4).

Experimental

General

All reactions were carried out under dry nitrogen, although normally no special precautions to exclude air were taken during subsequent work-up. Common solvents were dried, distilled under nitrogen and degassed before use. Separations were carried out by preparative thin-layer chromatography on glass plates ($20 \times 20 \text{ cm}^2$) coated with silica gel (Merck, 0.5 mm thick).

Instruments

IR spectra were obtained using a Bruker IFS28 FT-IR spectrometer. Spectra of CH_2Cl_2 solutions were obtained using a 0.5 mm path-length solution cell with NaCl windows. NMR spectra were recorded on a Varian Gemini 2000 instrument (^1H at 300.14 MHz, ^{13}C at 75.48 MHz, ^{31}P at 121.50 MHz). Unless otherwise stated, samples were dissolved in CDCl_3 contained in 5 mm sample tubes. Chemical shifts are given in ppm relative to internal tetramethylsilane for ^1H and ^{13}C NMR spectra, external H_3PO_4 for ^{31}P NMR spectra. Electrospray mass spectra (ES-MS) were obtained from samples dissolved in MeOH which, unless otherwise stated, contained NaOMe as an aid to ionisation.⁴⁴ Solutions were injected into a Varian Platform II spectrometer via a 10 ml injection loop. Nitrogen was used as the drying and nebulising gas. Peaks listed are the most intense of the isotopic clusters. Elemental analyses were by Campbell Microanalytical Laboratory, Chemistry Department, University of Otago, Dunedin, New Zealand.

Reagents

The compounds $\text{FeCl}(\text{dppe})\text{Cp}$,⁴⁵ $\text{RuCl}(\text{PPh}_3)_2\text{Cp}$,⁴⁶ $\text{Ru}(\text{C}\equiv\text{CPh})(\text{PPh}_3)_2\text{Cp}$,⁴⁶ *cis*- $\text{RuCl}_2(\text{dppe})_2$ ⁴⁷ and *trans*- $\text{PtCl}_2\{\text{P}(\text{tol})_3\}_2$ ⁴⁸ were all prepared by the cited literature procedures. All other reagents were obtained from Sigma-Aldrich or Fluka and used as received without further purification.

The compound $\text{Ru}\{\eta^3\text{-C}(\text{CN})_2\text{CPhC}=\text{C}(\text{CN})_2\}(\text{PPh}_3)\text{Cp}$ **1** was made as previously described from *tcne* and $\text{Ru}(\text{C}\equiv\text{CPh})(\text{PPh}_3)_2\text{Cp}$.¹¹ Crystals suitable for the X-ray study were obtained from $\text{MeCN-Et}_2\text{O}$. IR (Nujol cm^{-1}): $\nu(\text{CN})$ 2217 m; ($\text{CH}_2\text{Cl}_2/\text{cm}^{-1}$): $\nu(\text{CN})$ 2223 s. ^1H NMR: δ 4.80 (s, 5H, Cp), 7.30–7.55 (m, 20H, Ph). ^{13}C NMR: δ 7.9 [d, $J(\text{CP}) = 5 \text{ Hz}$, C(1)], 66.7 [d, $J(\text{CP}) = 2 \text{ Hz}$, C(2)], 84.9 [d, $J(\text{CP}) = 8 \text{ Hz}$, C(4)], 92.4

(s, Cp), 111.2 [d, $J(\text{CP}) = 3 \text{ Hz}$], 115.8 [d, $J(\text{CP}) = 3 \text{ Hz}$], 118.8 [d, $J(\text{CP}) = 7 \text{ Hz}$], 118.9 [d, $J(\text{CP}) = 1 \text{ Hz}$] ($4 \times \text{CN}$), 128.6–134.5 (m, Ph), 218.7 [d, $J(\text{CP}) = 15 \text{ Hz}$, C(3)]. ^{31}P NMR: δ 43.7 (s, PPh_3). Calculated ^{13}C NMR data for **1**: 17.3 [C(1)], 71.3 [C(2)], 81.6 [C(4)], 85.1 (Cp), 98.1 [C(6)N], 101.8 [CN at C(1) near Ru], 105.1 [CN at C(1) away from Ru], 105.4 [C(5)N], 111.5 (*meta* C, PPh_3), 112.3 [*meta* C at C(2)Ph], 113.3 [*para* C at C(2)Ph], 113.7 (*para* C, PPh_3), 114.2 [*ortho* C at C(2)Ph], 117.7 (*ipso* C, PPh_3), 118.1 (*ortho* C, PPh_3), 119.7 [*ipso* C at C(2)Ph], 208.9 [C(3)].

Reactions of $\text{Ru}\{\eta^3\text{-C}(\text{CN})_2\text{CPhC}=\text{C}(\text{CN})_2\}(\text{PPh}_3)\text{Cp}$ **1**

(a) **With NaOMe.** A solution of $\text{Ru}\{\eta^3\text{-C}(\text{CN})_2\text{-CPhC}=\text{C}(\text{CN})_2\}(\text{PPh}_3)\text{Cp}$ **1** (60 mg, 0.09 mmol) in thf-MeOH (5 : 1, 12 ml) was treated with NaOMe [from Na (0.11 mg) in MeOH (1 ml)] and the reaction mixture was stirred at r.t. for 48 h, during which time the colour changed from yellow to red-brown. After removal of solvent, a dichloromethane extract of the residue was separated by preparative t.l.c. (acetone–hexane, 3/7). A brown band (R_f 0.24) contained $\text{Ru}\{\text{NHC}(\text{OMe})\text{C}(\text{CN})=\text{CCPh}=\text{C}(\text{CN})_2\}(\text{PPh}_3)\text{Cp}$ **2** (46 mg, 72%), obtained as dark red crystals following recrystallisation from $\text{MeCN-Et}_2\text{O}$. Anal. Found: C, 65.80; H, 4.24; N, 8.15. Calcd ($\text{C}_{38}\text{H}_{29}\text{N}_4\text{OPRu}$): C, 66.88; H, 4.24; N, 8.12; M, 690. IR (cm^{-1}): $\nu(\text{CN})$ 2203 s, 2226 m; other bands at 1733 w (br), 1714 vw, 1607 m, 1579 s, 1520 m. ^1H NMR: δ 3.62 (s, 3H, OMe), 4.46 (s, 5H, Cp), 6.53 (s, 1H, NH), 6.67–7.53 (m, 20H, Ph). ^{31}P NMR: δ 46.9 (s, PPh_3). ES-MS (m/z): 713, $[\text{M} + \text{Na}]^+$.

(b) **With NaN_3 .** A suspension of **1** (100 mg, 0.15 mmol) and NaN_3 (20 mg, 0.3 mmol) in *dme* (50 ml) was heated under reflux for 24 h. Solvent was removed from the now dark red-purple solution and an acetone extract of the residue was purified by preparative t.l.c. (acetone–hexane, 2/1). The major red-purple band (R_f 0.20) contained $\text{Ru}\{\text{N}_3\text{N}[\text{Na}(\text{OEt}_2)]=\text{CC}(\text{CN})=\text{CCPh}=\text{C}(\text{CN})_2\}(\text{PPh}_3)\text{Cp}$ **3** (107 mg, 88%), obtained as very dark red crystals after recrystallisation from $\text{MeCN-Et}_2\text{O}$. Anal. Found: C, 62.03; H, 4.36; N, 11.88. Calcd ($\text{C}_{41}\text{H}_{35}\text{N}_7\text{NaOPRu}$): C, 61.81; H, 4.40; N, 12.31; M, 757. IR (cm^{-1}): $\nu(\text{CN})$ 2194 m, 2220 m; other bands at 1515 m (br), 1459 m (br), 1434 m, 1377 w. ^1H NMR (acetone- d_6): δ 1.12 (t, $J = 7 \text{ Hz}$, 6H, $2 \times \text{Me}$), 3.42 (q, $J = 7 \text{ Hz}$, 4H, $2 \times \text{CH}_2$), 4.33 (s, 5H, Cp), 7.09–7.50 (m, 20H, Ph). ^{13}C NMR (acetone- d_6): δ 15.0 (s, Me), 65.7 (s, CH_2), 72.3 [s, C(1)], 79.8 [d, $J(\text{CP}) = 2 \text{ Hz}$, Cp], 100.1 [s, C(4)], 115.6, 115.6, 116.7 ($3 \times$ s, CN), 127.9–134.0 (m, Ph), 168.3 [s, C(5)], 188.5 [s, C(2)], 221.0 [d, $J(\text{CP}) = 11 \text{ Hz}$, C(3)]. Calculated ^{13}C NMR data for anion of **3**: 64.5 [C(1)], 77.9 (Cp), 91.8 [C(4)], 102.3 [CN at C(1) near Ru], 103.3 [CN at C(4)], 104.5 [CN at C(1) away from Ru], 109.9 (*meta* C, PPh_3), 110.3 (*para* C, PPh_3), 110.5 [*meta* C at C(2)Ph], 110.9 [*para* C at C(2)Ph], 114.2 [*ortho* C at C(2)Ph], 118.1 (*ortho* C, PPh_3), 123.5 (*ipso* C, PPh_3), 123.6 [*ipso* C at C(2)Ph], 150.9 [C(5)], 160.1 [C(2)], 214.3 [C(3)]. ^{31}P NMR (acetone- d_6): δ 51.4 (s, PPh_3). ES-MS (negative ion, MeOH, m/z): 700, $[\text{M} - \text{Na}(\text{OEt}_2)]^-$; (positive ion, MeOH + NaOMe): 746 [anion + 2Na^+]; 724, [anion + (H + Na)]⁺. Both ions are weak, but the former increases in intensity upon addition of more NaOMe.

Three minor bands were also resolved, one of which afforded complex **4** (6 mg) (see below).

Reactions of $\text{Ru}\{\text{N}_3\text{N}[\text{Na}(\text{OEt})_2]=\text{CC}(\text{CN})=\text{CCPh}=\text{C}(\text{CN})_2\}-\text{(PPh}_3\text{)}_2\text{Cp}$

(a) With $\text{RuCl}(\text{PPh}_3)_2\text{Cp}$. A mixture of **3** (20 mg, 0.025 mmol) and $\text{RuCl}(\text{PPh}_3)_2\text{Cp}$ (18.1 mg, 0.025 mmol) was heated in refluxing dme (8 ml) for 30 min. Removal of solvent and purification of the residue by preparative t.l.c. (acetone–hexane, 1/2) gave a major purple band (R_f 0.30) which contained $\text{Ru}\{\text{N}_2\text{N}[\text{Ru}(\text{PPh}_3)_2\text{Cp}]\text{N}=\text{CC}(\text{CN})=\text{CCPh}=\text{C}(\text{CN})_2\}-\text{(PPh}_3\text{)}_2\text{Cp}$ **4** (32 mg, 91%), which formed dark red-brown crystals from CH_2Cl_2 . Anal. Found: C, 67.01; H, 4.89; N, 6.62. Calcd ($\text{C}_{78}\text{H}_{60}\text{N}_7\text{P}_3\text{Ru}_2$): C, 67.38; H, 4.35; N, 7.05; M, 1391. IR (cm^{-1}): $\nu(\text{CN})$ 2203 m, 2221m; other bands at 1729 w (br), 1516 m, 1501 m, 1482 m. $^1\text{H NMR}$: δ 3.95 (s, 5H, Cp), 4.05 (s, 5H, Cp), 6.89–7.32 (m, 50H, Ph). $^{31}\text{P NMR}$: δ 45.0 [d, $J(\text{PP}) = 4$ Hz, 2P, PPh_3], 47.4 (s, 1P, PPh_3). ES-MS (m/z): 1415, $[\text{M} + \text{H} + \text{Na}]^+$; 1392, $[\text{M} + \text{H}]^+$.

(b) With $\text{FeCl}(\text{dppe})\text{Cp}$. A similar experiment used **3** (20 mg, 0.025 mmol), $\text{FeCl}(\text{dppe})\text{Cp}$ (14 mg, 0.025 mmol) in dme (8 ml), heating for 1.5 h. Preparative t.l.c. (acetone–hexane, 3/7) gave a purple band (R_f 0.19) containing $\text{Ru}\{\text{N}_2\text{N}[\text{Fe}(\text{dppe})\text{Cp}]\text{N}=\text{CC}(\text{CN})=\text{CCPh}=\text{C}(\text{CN})_2\}-\text{(PPh}_3\text{)}_2\text{Cp}$ **5** (23 mg, 76%) as dark red crystals after recrystallisation from CH_2Cl_2 –MeOH. Anal. Found: C, 66.75; H, 4.45; N, 7.90. Calcd ($\text{C}_{68}\text{H}_{54}\text{FeN}_7\text{P}_3\text{Ru}$): C, 67.00; H, 4.45; N, 8.04; M, 1219. IR (cm^{-1}): $\nu(\text{CN})$ 2198 m, 2221 m; other bands at 1514 m, 1481 m, 1311 w. $^1\text{H NMR}$: δ 2.33, 2.82 (2 \times m, 2 \times CH_2 , dppe), 3.97 (s, 5H, Cp–Ru), 4.27 [s (br), 5H, Cp–Fe], 6.64–7.45 (m, 40H, Ph). $^{31}\text{P NMR}$: δ 42.2 (s, 1P, PPh_3), 108.0 [s (br), 2P, dppe]. ES-MS (m/z): 1242, $[\text{M} + \text{Na}]^+$; 1219, M^+ .

(c) With $\text{trans-PtCl}_2\{\text{P}(\text{tol})_3\}_2$. A mixture of **3** (32 mg, 0.4 mmol) and $\text{trans-PtCl}_2\{\text{P}(\text{tol})_3\}_2$ (35 mg, 0.04 mmol) was heated in refluxing dme (25 ml) for 6 h. After removal of solvent, an acetone extract of the residue was purified by preparative t.l.c. (acetone–hexane, 1/2) to give a major purple-red band (R_f 0.48) containing $\text{Ru}\{\text{N}_3\text{N}[\text{cis-PtCl}_2\{\text{P}(\text{tol})_3\}_2]=\text{CC}(\text{CN})=\text{CCPh}=\text{C}(\text{CN})_2\}-\text{(PPh}_3\text{)}_2\text{Cp}$ **6** (45 mg, 74%), isolated as red-brown crystals after recrystallisation from CH_2Cl_2 –MeOH. Anal. Found: C, 60.93; H, 4.39; N, 6.25. Calcd ($\text{C}_{79}\text{H}_{67}\text{ClN}_7\text{P}_3\text{PtRu}$): C, 61.66; H, 4.39; N, 6.37; M (unsolvated), 1539. IR (cm^{-1}): $\nu(\text{CN})$ 2199 w, 2222 w; other bands at 1520 m, 1464 m, 1437 m, 1379 w. $^1\text{H NMR}$: δ 2.32 (s, 18H, Me), 4.10 (s, 5H, Cp), 5.31 (s, 2H, CH_2Cl_2), 6.96–7.21 (m, 44H, Ph + C_6H_4). $^{13}\text{C NMR}$: δ 21.4 (s, Me), 71.6 [C(1)], 79.8 (s, Cp), 97.2 [C(4)], 114.4, 114.9, 116.3 (3 \times s, CN), 125.2–135.2 (m, Ph + C_6H_4), 185.9 [C(2)], C(3) and C(5) peaks are not observed. Calculated $^{13}\text{C NMR}$ data for **6**: 17.3–17.5 (Me), 77.4 (Cp), 87.2 [C(4)], 101.4 [CN at C(1) near Ru], 103.1 [CN at C(1) away from Ru], 106.5 [CN at C(4)], 108.8–129.2 (aromatic Cs), 147.3 [C(5)], 158.9 [C(2)], 239.4 [C(3)]. $^{31}\text{P NMR}$: δ 4.0 [d, $J(\text{PP}) = 19$ Hz, $J(\text{PPt}) = 3322$ Hz, 2P, $\text{P}(\text{tol})_3$], 14.3 [d, $J(\text{PP}) = 19$ Hz, $J(\text{PPt}) = 3322$ Hz, $\text{P}(\text{tol})_3$], 39.9 (s, PPh_3). ES-MS (m/z): 1562, $[\text{M} + \text{Na}]^+$.

(d) With MeOTf. A suspension of **3** (20 mg, 0.025 mmol) in thf (7 ml) was treated with MeOTf (4 mg, 0.025 mmol) dissolved in thf (1 ml). After keeping at r.t. for 1 h, solvent was removed and an acetone extract of the residue was separated by preparative t.l.c. (acetone–hexane 2/3). The red-purple baseline contained unreacted **3** (13 mg, 67%) and an orange band (R_f 0.70) which afforded an oil. Purification of this oil multiple times by

t.l.c. afforded $\text{Ru}\{\text{N}_3\text{NMe}=\text{CC}(\text{CN})=\text{CCPh}=\text{C}(\text{CN})_2\}-\text{(PPh}_3\text{)}_2\text{Cp}$ **7** (4 mg, 24%) as red crystals from CHCl_3 –MeOH. Anal. Found: C, 63.11; H, 3.97; N, 13.56. Calcd ($\text{C}_{38}\text{H}_{28}\text{N}_7\text{PRu}$): C, 63.86; H, 3.95; N, 13.72; M, 715. IR (cm^{-1}): $\nu(\text{CN})$ 2199 m, 2224 m; other bands at 1556 m, 1520 m, 1462 w, 1401 w. $^1\text{H NMR}$: δ 3.89 (s, 3H, Me), 4.75 (s, 5H, Cp), 7.15–7.36 (m, 20H, Ph). $^{31}\text{P NMR}$: δ 49.5 (s, PPh_3). ES-MS (positive ion, MeOH + NaOMe, m/z): 1453, $[2\text{M} + \text{Na}]^+$; 738, $[\text{M} + \text{Na}]^+$.

(e) With $\text{cis-RuCl}_2(\text{dppe})_2$. A reaction between **3** (20 mg, 0.025 mmol) and $\text{cis-RuCl}_2(\text{dppe})_2$ (12.1 mg, 0.0125 mmol) was carried out in refluxing dme (20 ml) for 14 h. The usual work-up (acetone–hexane 3/7) afforded recovered **3** (7 mg, 35%) together with an orange band (R_f 0.14) from which $\text{Ru}\{\text{N}_2\text{N}[\text{CH}(\text{CH}_2\text{OMe})(\text{OMe})]\text{N}=\text{CC}(\text{CN})=\text{CCPh}=\text{C}(\text{CN})_2\}-\text{(PPh}_3\text{)}_2\text{Cp}$ **8** (3.4 mg, 17%) was obtained as red-brown crystals from CH_2Cl_2 –MeOH. Anal. Found: C, 62.17; H, 4.23; N, 12.69. Calcd ($\text{C}_{41}\text{H}_{34}\text{N}_7\text{O}_2\text{PRu}$): C, 62.43; H, 4.34; N, 12.43; M, 790. IR (cm^{-1}): $\nu(\text{CN})$ 2197 m, 2223 m; other bands at 1728 w (br), 1533 m, 1515 m, 1478 m, 1354 m, 1195 m. ES-MS (m/z): 1603, $[2\text{M} + \text{Na}]^+$; 812, $[\text{M} + \text{Na}]^+$; 790, M^+ .

(f) Independent preparation of **8 and its isomer **9**.** A solution of **3** (10.5 mg, 0.013 mmol) in dme (5 ml) was heated at reflux point for 48 h, the colour of the solution gradually changing from purple to brown-red. The filtered solution was evaporated under vacuum and the residue was dissolved in acetone and separated by preparative t.l.c. (acetone–hexane, 3/7) to give two bands. The first orange band (R_f 0.16) contained **9** (1 mg, 13%), obtained as red crystals from CH_2Cl_2 –EtOH. The second orange band (R_f 0.14) afforded **8** (2 mg, 21%) as brown-red crystals after recrystallisation from CH_2Cl_2 –EtOH.

Structure determinations

The crystal data for **1–9** are summarised in Table 3 with the structures depicted in Fig. 1–8, where ellipsoids have been drawn at the 50% probability level (20% for **5**) and hydrogen atoms have arbitrary radii of 0.1 Å. Selected coordination geometries for **2–9** are given in Table 1. Crystallographic data for the structures were collected at low temperature (T/K quoted) on Oxford Diffraction Gemini (for **1**, **5**, **6**, **9**) or Xcalibur diffractometers (for **2–4**, **7**, **8**) fitted with monochromated Mo $\text{K}\alpha$ ($\lambda = 0.71073$ Å; **2–4**, **7–9**) or Cu $\text{K}\alpha$ radiation ($\lambda = 1.54178$ Å; **1**, **5**, **6**) yielding N_{tot} reflections, merging to N unique after multi-scan (**2–5**, **9**) or face-indexed (**1**, **6–8**) absorption corrections (R_{int} cited), with N_o reflections having $I > 2\sigma(I)$. The structures were refined against F^2 with full-matrix least-squares using the program SHELXL-97.^{49a} In general, all H atoms were added at calculated positions and refined by use of a riding model with isotropic displacement parameters based on the isotropic displacement parameter of the parent atom. Exceptions were in **2** where H(52) was refined without restraints. Anisotropic displacement parameters, except where stated, were employed for all non-hydrogen atoms. For **6**, the occupancy factor for the CH_2Cl_2 solvent molecule refined to 0.160(8), this being reflected in the large mosaic spread and weak diffraction. The solvent C atom was refined with an isotropic displacement parameter only. For **7**, the water molecule H geometries were restrained to ideal values. For **8**, one MeO group of the coordinated dme ligand was modelled as being disordered over two sites with refined site

Table 3 Crystal data and refinement details

Complex	1	2	3	4	5	6	7	8	9
Formula	C ₃₇ H ₂₅ N ₄ PRu	C ₃₈ H ₂₉ N ₄ -OPRu	C ₄₁ H ₃₃ N ₇ -NaOPRu	C ₇₈ H ₆₀ N ₇ -P ₃ Ru ₂	C ₆₈ H ₅₄ FeN ₇ -P ₃ Ru	C ₇₀ H ₆₅ ClN ₇ -P ₃ PtRu-0.16CH ₂ Cl ₂	C ₃₈ H ₂₈ N ₇ -PRu·H ₂ O	C ₄₁ H ₃₄ N ₇ O ₂ -PRu-0.3CH ₂ O	C ₄₁ H ₃₄ N ₇ -O ₂ PRu
MW	657.65	689.69	796.79	1390.38	1219.01	1552.5	732.73	798.4	788.79
Crystal system	Monoclinic	Monoclinic	Monoclinic	Triclinic	Monoclinic	Monoclinic	Monoclinic	Triclinic	Monoclinic
Space group	<i>P</i> ₂ / <i>c</i>	<i>P</i> ₂ / <i>c</i>	<i>P</i> ₂ / <i>c</i>	<i>P</i> $\bar{1}$	<i>P</i> ₂ / <i>c</i>	<i>P</i> ₂ / <i>n</i>	<i>P</i> ₂ / <i>n</i>	<i>P</i> $\bar{1}$	<i>P</i> ₂ / <i>n</i>
<i>a</i> /Å	8.7167(1)	10.1827(1)	19.5078(8)	12.6767(4)	11.8912(3)	17.9190(3)	13.5236(3)	12.5756(4)	12.3947(2)
<i>b</i> /Å	17.6764(2)	19.0790(2)	9.6382(2)	15.6939(5)	32.4015(10)	18.4210(3)	13.7074(3)	13.0641(6)	17.7047(3)
<i>c</i> /Å	19.8463(2)	16.4900(1)	22.4454(9)	18.7018(7)	15.3484(4)	22.6747(4)	17.8548(3)	13.7818(5)	17.1249(3)
α /°				102.871(3)				64.569(4)	
β /°	99.231(1)	104.380(1)	115.464(5)	104.493(3)	99.774(3)	105.141(2)	98.452(2)	69.109(3)	97.322(2)
γ /°				90.705(3)				66.706(4)	
<i>V</i> /Å ³	3018.3	3103.2	3810.2	3502.6	5827.8	7224.8	3273.9	1829.9	3727.3
ρ_c	1.447	1.476	1.389	1.318	1.389	1.427	1.487	1.449	1.406
<i>Z</i>	4	4	4	2	4	4	4	2	4
$2\theta_{\max}$ /°	134 (0.60)	82 (0.92)	58 (0.68)	68 (0.79)	136 (0.60)	134 (0.60)	69 (0.80)	72 (0.83)	65 (0.76)
($\sin\theta$)/ λ_{\max}									
μ /mm ⁻¹	4.96	0.60	0.51	0.55	5.25	6.71	0.57	0.52	0.51
<i>T</i> _{min/max}	0.67/0.83	0.84/0.91	0.72/1.0	0.98/1.0	0.35/1.0	0.53/0.83	0.86/0.96	0.85/0.99	0.87/0.95
Crystal dimensions/mm ³	0.11 × 0.11 × 0.05	0.31 × 0.23 × 0.15	0.21 × 0.15 × 0.05	0.14 × 0.13 × 0.08	0.22 × 0.17 × 0.04	0.14 × 0.11 × 0.03	0.40 × 0.32 × 0.09	0.66 × 0.13 × 0.02	0.22 × 0.14 × 0.10
<i>N</i> _{tot}	30 233	85 683	47 404	74 235	73 154	81 172	52 868	40 379	42 565
<i>N</i> (<i>R</i> _{int})	5340 (0.078)	20 107 (0.044)	10 103 (0.063)	27 609 (0.053)	10 360 (0.12)	12 778 (0.093)	13 247 (0.063)	16 687 (0.041)	12 675 (0.068)
<i>N</i> _o	4429	11 897	6251	14 417	5010	7969	8224	10 462	7571
<i>R</i> ₁	0.037	0.033	0.050	0.042	0.085	0.054	0.045	0.045	0.037
w <i>R</i> ₂	0.097	0.095	0.122	0.082	0.278	0.162	0.100	0.117	0.073
<i>T</i> /K	100	150	100	100	200	100	100	100	100

occupancy factors of 0.628(5) and 1–0.628(5). Two close atoms were modelled as being the C and O atoms of a solvent MeOH molecule with site occupancy refining to 0.298(6). Solvent H atoms were not included in the model. Atoms of the minor component of the disordered dme and of the solvent molecule were refined with isotropic displacement parameters.

Both **4** and **6** contain voids. Those in **4** are large but, as recorded in the cif, no significant e-density was located. Use of the program SQUEEZE did significantly decrease the *R*-factor. For **6**, the voids are small and program SQUEEZE was not used.

The Table of Contents graphic was generated from the molecular structure of **1** using the OLEX2 suite of programs.^{49b}

Computational section

All DFT computations were carried out with the Gaussian 03 package.⁵⁰ The geometries of **1**, **3**, **5**, **6**, **10** and **11** discussed here were optimised at the B3LYP^{51,52}/3-21G*⁵³ (LANL2DZ⁵⁴ for Pt in **6**) level of theory with no symmetry constraints. Wiberg bond indices, atomic bond orbitals and natural charges were computed with the NBO 3.1 version. Electronic structure calculations were also carried out at the B3LYP/3-21G* level of theory. The MO diagrams and orbital contributions were generated with the aid of Gabedit⁵⁵ and GaussSum⁵⁶ packages respectively. Theoretical ¹³C NMR chemical shifts obtained at the GIAO^{57,58}-B3LYP/3-21G**/B3LYP/3-21G* level on the optimised geometries were referenced to TMS: $\delta(^{13}\text{C}) = 200 - \sigma(^{13}\text{C})$. Computed NMR values reported here for phenyl, methyl and Cp groups are averaged.

Frequency calculations on the optimised model geometries of **1** and **3** with Ph groups replaced by H atoms with the

basis set 3-21G* or the larger mixed basis set LANL2DZ/6-31G* (LANL2DZ for Ru, 6-31G* for other atoms) revealed no imaginary frequencies. Geometrical differences were insignificant between these model geometries at both basis sets indicating the 3-21G* basis set to be appropriate for computations on compounds **1**, **3**, **5**, **6** and **8–11** discussed here. The 3-21G* basis set was also found to be suitable for related ruthenium complexes discussed elsewhere.^{59–62} Calculated charges at NBO 3.1 on these model geometries were found to be basis set-independent on going from 3-21G* to LANL2DZ/6-31G* with only the positive charge at the ruthenium atom being significantly smaller with the LANL2DZ basis set.

Acknowledgements

We thank the Australian Research Council for support of this work and Johnson Matthey plc for a generous loan of RuCl₃·*n*H₂O. Mass spectra were obtained by Professor B. K. Nicholson (Department of Chemistry, Waikato University). We thank Durham University for access to the High Performance Computing Cluster.

References

- A. Davison and J. P. Solar, *J. Organomet. Chem.*, 1979, **166**, C13.
- M. I. Bruce, T. W. Hambley, M. R. Snow and A. G. Swincer, *Organometallics*, 1985, **4**, 494.
- M. I. Bruce, T. W. Hambley, M. R. Snow and A. G. Swincer, *Organometallics*, 1985, **4**, 501.
- M. I. Bruce, D. N. Duffy, M. J. Liddell, M. R. Snow and E. R. T. Tiekink, *J. Organomet. Chem.*, 1987, **335**, 365.

